OCS Study
MMS 2006-009

Transport over the Inner-Shelf of the Santa Barbara Channel

Final Technical Summary

Final Study Report

U.S. Department of the Interior
Minerals Management Service
Pacific OCS Region

OCS Study
MMS 2006-009

Transport over the Inner-Shelf of the Santa Barbara Channel

Final Technical Summary

Final Study Report

Author

J. Carter Ohlmann
Principal Investigator

Prepared under MMS Cooperative
Agreement No. 1435-01-00-CA-31063
by
Coastal Marine Institute
Marine Science Institute
University of California
Santa Barbara, CA 93106-6150

U.S. Department of the Interior
Minerals Management Service
Pacific OCS Region

Camarillo
February 2006

Disclaimer

This report has been reviewed by the Pacific Outer Continental Shelf Region, Minerals Management Service, U.S. Department of the Interior and approved for publication. The opinions, findings, conclusions, or recommendations in this report are those of the authors, and do not necessarily reflect the views and policies of the Minerals Management Service. Mention of trade names or commercial products does not constitute an endorsement or recommendation for use. This report has not been edited for conformity with Minerals Management Service editorial standards.

Availability of Report

Extra copies of the report may be obtained from:

U.S. Dept. of the Interior
Minerals Management Service
Pacific OCS Region
770 Paseo Camarillo
Camarillo, CA 93010
Phone: 805-389-7621

A PDF file of this report is available at:
http://www.coastalresearchcenter.ucsb.edu/CMI/

Suggested Citation

The suggested citation for this report is:

J. Carter Ohlmann. Transport over the Inner-Shelf of the Santa Barbara Channel. MMS OCS Study 2006-009. Coastal Research Center, Marine Science Institute, University of California, Santa Barbara, California. MMS Cooperative Agreement Number 1435-01-00-CA-31063. 29 pages.

Table of Contents

List of Tables

List of Figures

FINAL TECHNICAL SUMMARY

STUDY TITLE: Transport over the Inner-Shelf of the Santa Barbara Channel

REPORT TITLE: Transport over the Inner-Shelf of the Santa Barbara Channel

CONTRACT NUMBER: 1435-01-00-CA-31063

SPONSORING OCS REGION: Pacific

APPLICABLE PLANNING AREA(S): Southern California

FISCAL YEAR(S) OF PROJECT FUNDING: FY 01, FY 02

COMPLETION DATE OF REPORT: April 2005

COSTS: FY 01 - $97,480; FY 02 - $87,032

CUMULATIVE PROJECT COST: $184,512

PROJECT MANAGERS: Russell J. Schmitt

AFFILIATION: Coastal Research Center, Marine Science Institute, University of California, Santa Barbara, CA 93106

ADDRESS: University of California, Santa Barbara, CA 93106-6150

PRINCIPAL INVESTIGATOR: J. Carter Ohlmann

ADDRESS: Institute for Computational Earth System Science, University of California, Santa Barbara, CA 93106

KEY WORDS: Ocean circulation, drifting buoys, radar data, Lagrangian circulation

BACKGROUND: Existing studies in the Santa Barbara Channel have focused on the basin scale circulation, but little is known about ocean currents over the inner-shelf.

OBJECTIVES: Descriptive and statistical views of regional circulation, examination of small-scale flow patterns unresolved in H.F. radar data, and investigation of the accuracy of particle paths determined from Eulerian H.F. radar fields.

DESCRIPTION: A total of 17 deployments over the inner-shelf off the Santa Barbara coast during 2003 with a fleet of 15 drifters yielded 171 drifter tracks. Additionally, drifters were repetitively deployed within a 2 km square HF radar grid located further offshore giving 128 much shorter tracks.

SIGNIFICANT CONCLUSIONS/ STUDY RESULTS: The inner-shelf drifters generally move up-coast and on-shore, in opposition to the prevailing direction of wind forcing, with mean velocities between 3.5 and 34.5 cm s^{-1}. This suggests that pressure and/or Coriolis forces may play significant roles in the local dynamics. Velocity variance is near the same order as mean values indicating the importance of high frequency fluctuations in the region. Comparisons between drifter and HF radar velocities indicate that rms differences decrease from ~10 to ~6 cm s^{-1} when the number of drifter observations in an HF radar bin increases to more than 30. This result is supported by EKE computations which demonstrate increased energy with more drifter observations. Thus, motions on scales not resolved with HF radar observations are a significant component of the local circulation. Comparison between observed drifter tracks and tracks computed with Eulerian HF radar fields shows the two diverge at rates of roughly 5 and 9 cm sec^{-1} in the along- and across-shore directions, respectively. Knowledge of such directional biases is necessary for developing sub-grid-scale parameterizations to be used with HF radar fields for accurately determining pathways in the coastal ocean.

STUDY PRODUCTS:

Publications:

Ohlmann, J. C., P.F. White, A. L. Sybrandy, and P. P. Niiler, GPS-Cellular drifter technology for coastal ocean observing systems, *Journal of Atmospheric and Oceanic Technology*, in press.

Ohlmann, J. C., and P. F. White, Lagrangian circulation characteristics over the inner shelf of the Santa Barbara channel. In preparation for Continental Shelf Research

Research Presentations:

Presentations were made at the TOS and LAPCOD meetings held during the summer of 2005.

FINAL STUDY REPORT

1. Introduction

The Santa Barbara Channel (SBC) exhibits two primary characteristics that continually prompt regional oceanographic studies. First, the Channel contains significant natural oil and gas resources, including one of the world's largest natural hydrocarbon seeps, and commercial operations. The fate of naturally seeping hydrocarbons and potentially leaked or spilled oil is of interest. Second, the location of the SBC at the northern edge of the Southern California Bight leads to ecological diversity, as both northern and southern species exist. Understanding larvae transport pathways is necessary for sound ecological management. The Channel Islands National Marine Sanctuary (a marine protected area; http://channelislands.noaa.gov/), and the United States Minerals Management Service (MMS) Rigs-to-Reefs conversions are specific examples of local ecological programs.

The SBC is roughly 100 km long by 50 km wide, is oriented in the east-west direction, and is located at the northern edge of the Southern California Bight. Four Channel Islands comprise the southern boarder. Narrow continental shelves extend ~5 km offshore along both the northern and southern boundaries. Water depth in the center of the channel reaches 600 m. Complicated bathymetry, a highly variable wind field, and strong spatial gradients also characterize the channel (e.g. Dorman and Winant 2000). Three year mean SST and current velocity values just beyond the northwestern edge of the channel are 13 C and 20 cm s^{-1}, respectively. Corresponding SST and surface velocity values at the eastern end are 16 C and 5 cm s^{-1} (Harms and Winant 1998).

Ocean circulation studies in the Channel have been ongoing since at least the significant 1969 oil spill. Using drift cards and hydrographic surveys, Kolpack (1971) observed a cyclonic gyre in the western half of the Channel and northwesterly flow in the east Channel. Current meter data, collected from April – June 1983, at 13 locations around the periphery of the Channel, confirmed part of the Kolpack gyre (Brink and Muench 1986). Time varying currents were found to not necessarily be related to local wind forcing as in other California coastal regions (e.g. Davis 1985, Lenz and Winant 1986, Lenz 1994).

A more comprehensive observational program that extended northward into the Santa Maria basin (SMB) was carried out in the 1990s. Eight moorings were deployed around the perimeter of the SBC for near 3 years (generally 1993 to 1996). In addition, 347 surface drifters were deployed in the SBC-SMB region between mid-1993 and the end of 1999. The mooring data were used to present the large scale SBC circulation in terms of 6 characteristic patterns that develop in response to wind and sea level forcing (Harms and Winant 1998). Statistical analysis of the Argos tracked drifter data provide a more complete spatial description of the 6 patterns and indicate Lagrangian time and space scales of 1 day and less than 10 km (Dever et al. 1998). Small scale flow features tracked by the drifters have been described by Winant et al. (1999). The 6 large scale patterns have been reduced to 3 over an increased spatial domain (Winant et al. 2003). The modeling study of Oey et al. (2001) indicates the dominant modes arise from an imbalance between a mostly westward sea level gradient, a mostly eastward wind stress, and

Coriolis. Oey et al. (2001) give 2 circulation regimes; 1 during winds of nearly equal strength throughout the SBC, and 1 for a strong along-channel wind gradient.

The existing SBC circulation studies have focused on the basin scale. Current meter moorings and drifter releases have typically been along the 100 m isobath, or deeper, throughout the Channel. Service Argos tracked drifters sample roughly 4 or 5 times daily with spatial accuracy of order 100 meters or more. Surface drifters eventually sample the inner-shelf region (depths < ~100 m) but with coarse resolution. The discrepancy in scale has led Dever et al. (1998) to completely disregard drifter observations collected near the coast. High frequency Doppler radar (HF radar) data exists for the SBC (Beckenbach and Washburn 2004) but necessary averaging gives hourly data on a 2 km grid, which is also too coarse to resolve inner-shelf dynamics (Ohlmann et al. in press). Additionally, CODAR data is suspect in the near-shore region where beam direction becomes mostly aligned with wave crests and the deep-water wave approximation is violated (Graber et al. 1997).

The objective of this research is to describe and quantify the surface velocity field over a portion of the SBC inner-shelf with high-resolution Lagrangian drifters. Inner-shelf dynamics are important for determining the fate of larvae, often spawned very near the coast. The economic detriment of oil and other pollutants primarily occurs when the contaminants reach the surf-zone, which requires passing over the inner shelf region. Drifters give direct information about pathways of passive tracers and provide Lagrangian data which allows achievement of the following:

- Descriptive and statistical views of regional circulation.
- Examination of small-scale flow patterns unresolved in HF radar data.
- Investigation of the accuracy of particle paths determined from Eulerian fields.

This is the first inner-shelf drifter study known to utilize data with such high resolution in time and space collected over the course of a year. Results should pave the way for more comprehensive programs, involving expanded observations and a modeling component, with the goal of identifying the roles of the various forcing mechanisms and dynamical quantities and accurately forecasting the flow field.

2. Coastal drifter (instrumentation)

2.1 Design

Development of a drifter suitable for use in the coastal ocean is the first component of this research. Coastal drifters must be small and space efficient for transport and deployment from small boats, and must be economical so they can be deployed in large numbers. In addition, they must have spatial resolution of a few meters, and sample their position every few minutes to properly resolve characteristic scales of inner-shelf motions. Near-real-time data telemetry is required so the drifters can be used to aid in the tracking and recovery of missing objects, and for recovery of the drifters themselves without visual monitoring. Recoverability and redeployment greatly enhances drifter economy. Drifter electronics must be suitably energy efficient so they can sample and transmit every few minutes for a number of days at a time.

A corner-radar-reflector type drogue was selected for the coastal drifter for two primary reasons (Figure 1). First, this is a known calibrated drag element in existing use (Niiler et al. 1995). Second, the design allows the drogue to be collapsed so that a large number can be stowed on, and deployed from, a small (20 ft) skiff. A surface float houses all the drifter electronics, and provides buoyancy so that the droque remains centered at a depth of 1 m. The spherical shape minimizes drifter slip due to surface wave forcing.

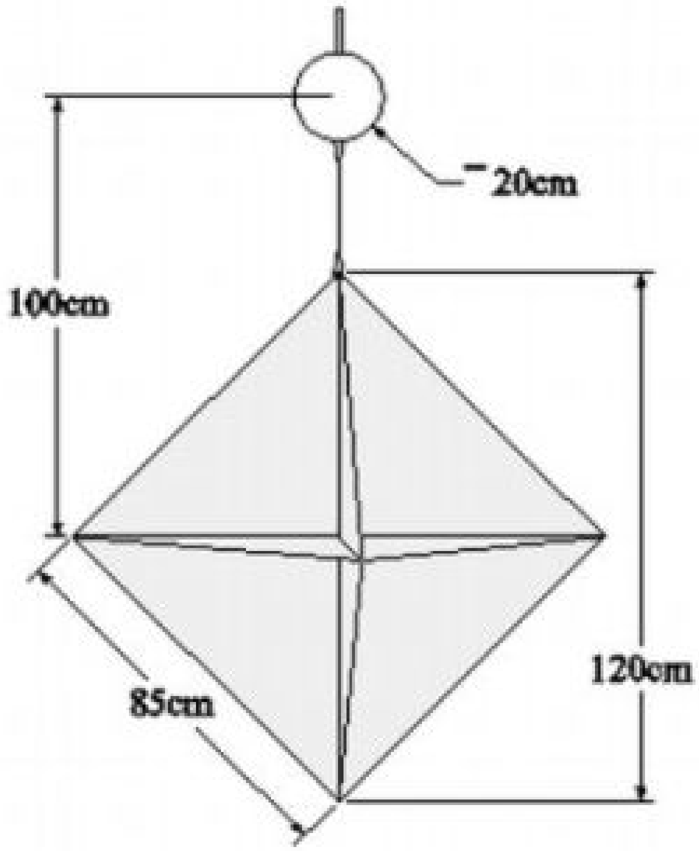

Figure 1. Schematic of the coastal drifter.

Drifter position is obtained with GPS technology. GPS gives position data with the highest spatial and temporal resolution at the lowest possible cost. Data transmission in near-real-time can be carried out through either satellite or cellular systems. Satellite allows for large area coverage but comes at significant cost. Cellular systems require that drifters sample within a limited line-of-sight radius of cellular base stations. However, cellular communications costs are near $0.50 per drifter-day for 10 minute position records, and there are few restrictions on the quantity of data that can be transmitted. The Mobitex (www.mobitex.org) cellular communications system was selected for data transmission. Mobitex is a packet-switched, narrowband, data-only technology ideally suited for applications such as interactive messaging, e-mail, telemetry, telematics/positioning, alarms, and forms-based transmissions. It allows for two-way communications so drifters can be commanded remotely. Cellular coverage is excellent in coastal southern California, from Point Conception to the Mexican border within ~40 km of the shore. Data records transmitted across the Mobitex network are received by a host computer continuously connected to the Web, allowing near-real-time data to be accessed from any computer connected to the Internet.

A map-based drifter monitoring software system developed in Matlab facilitates drifter management (Figure 2). The Matlab Coastal Drifter Tracking Software (CDTS) was developed to monitor movement so drifters could be retrieved prior to leaving a study region (including beaching). Viewing the relative positions of all drifters on a map also facilitates an efficient order of recovery. The CDTS obtains drifter data from the host computer every minute, or upon user request, and displays the drifter positions on a map, and detailed information in a 7-column table. Tracks can be toggled on and off both the tabular and map displays.

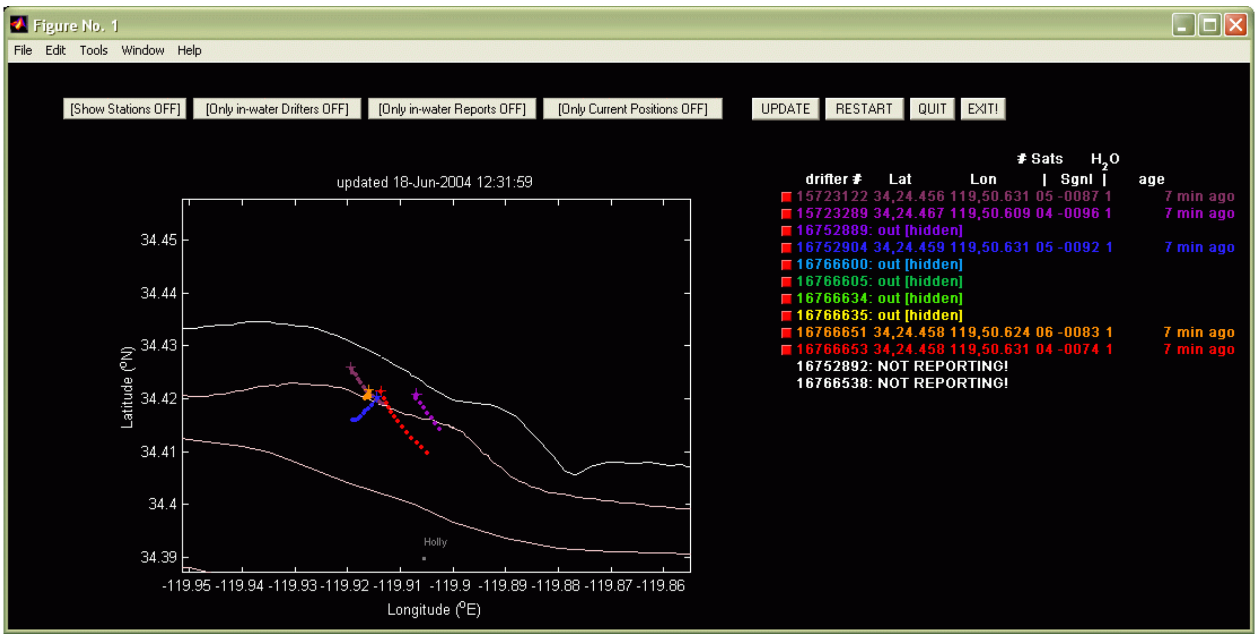

Figure 2. Coastal drifter tracking software screen. The interactive software displays tracks for selected drifters, along with status data for the entire fleet. Drifter tracks to be displayed are selected by toggling the drifter identification number. "out [hidden]" on the status table indicates the drifter is sampling but its track is not being displayed on the map. "NOT REPORTING!" indicates the drifter is not activated. The screen shows data collected on 6 December 2002, played back on 18 June 2004.

2.2 Performance

To test the variance in GPS position data, a set of 14 drifters were activated in fixed positions. Each drifter obtained position data every 10 minutes for nearly 2 days (269 position records per unit). Standard deviation in position for each of the 14 drifters ranges from 2.9 to 6.8 m. The overall standard deviation for all drifters is 4.06 m.

To quantify water-following characteristics, a drifter was configured with a pair of Nortek Aquadopp acoustic current meters, located at the top and bottom of the drogue. Drifter slip, which gives the rate and direction that water parcels slip by the drifter, was computed as the mean of the upper and lower Aquadopp velocities. Results of 6 Aquadopp-drifter deployments are summarized in Table 1. Slip ranges from 0.22 to 2.04 cm s^{-1} in relatively calm wind and wave conditions. The smallest slip values occur during times when the average wind speed over the deployment period is < 1 m s^{-1}, and significant wave height is < 1 m. The largest slip values occur in the roughest conditions encountered, and nearest the shore where the steepest waves are expected.

Table 1. Summary of Aquadopp-drifter deployments. Values are means over each deployment lasting ~30 minutes. Aquadopp current quantities (Upper, Lower, Slip, and Shear) are given as a velocity followed by the direction of motion. Wind and Wave values are given as the direction they are coming from. Slip is computed as the average of the upper and lower mean Aquadopp velocity vectors. Shear is the difference between the mean velocity vectors (lower-upper). Wind values are from the NOAA East Santa Barbara Channel buoy. Wave height and direction are from local estimates.

Deployment Date	Water Depth (m)	Upper Velocity (cm s^{-1}) (degrees)	Lower Velocity (cm s^{-1}) (degrees)	Slip (cm s^{-1}) (degrees)	Shear (cm s^{-1}) (degrees)	Wind (m s^{-1}) (degrees)	Waves (m) (degrees)	Drifter Movement (cm s^{-1}) (degrees)
6 Aug 2004	15	0.15 183	1.03 240	0.56 234	0.96 247	< 1 315	< 1 210	7 330
18 Aug 2004	90	1.00 61	2.73 203	1.02 185	3.57 213	2.0 299	< 1 210	30 185
31 Aug 2004	5	0.68 146	0.79 68	0.57 103	0.94 22	< 1 228	< 1 230	6 352
31 Aug 2004	125	0.23 179	0.21 184	0.22 181	0.03 318	< 1 228	< 1 280	14 39
13 Sept 2004	5	1.72 233	2.56 198	2.04 211	1.54 157	2.5 270	1.0 225	13 324
13 Sept 2004	25	0.32 131	2.96 229	1.47 222	3.01 234	2.5 270	1.0 245	77 315

The drifter slip analysis indicates the presence of vertical shear extending over the vertical distance of the drogue (0.45 to 1.55 m beneath the surface). The shear profile is not necessarily uniform. Velocity measurements at the top and bottom of the drogue may not accurately integrate the velocity over the entire drogue, resulting in a perceived, rather than actual, slip. This integration effect, combined with the small slip values, suggests the drifters follow the mean flow over the drogue area to within ~1-2 cm s^{-1}. During deployments demonstrating a slip larger than 1 cm s^{-1}, the slip is aligned (180° out of phase) with the wave stress to within 25°, suggesting surface waves are "pushing" the drifter through water.

Results of the limited Aquadopp-drifter tests show that slip values are less than ~2 cm s^{-1} during relatively calm conditions, consistent with results given in Davis (1985) for a similar drogue design. The data are insufficient for demonstrating clear relationships with wind speed and significant wave height. A further understanding of slip requires sampling in a wider range of conditions and a better understanding of vertical shear over the drogue depth. In the meantime, slip quantification allows the data to be properly interpreted.

3. Experimental design

3.1 Study region

Inner-shelf surface currents in the region near Coal Oil Point (Figure 3) are being studied. This is a location of active natural oil and gas seepage, and has been the site of numerous MMS funded field studies. The region is located within the SBC high frequency (HF) radar sampling domain, and is near the routinely sampled Naples reef LTER study site. The location is also within a few miles of the Goleta pier boat launch and the UCSB campus.

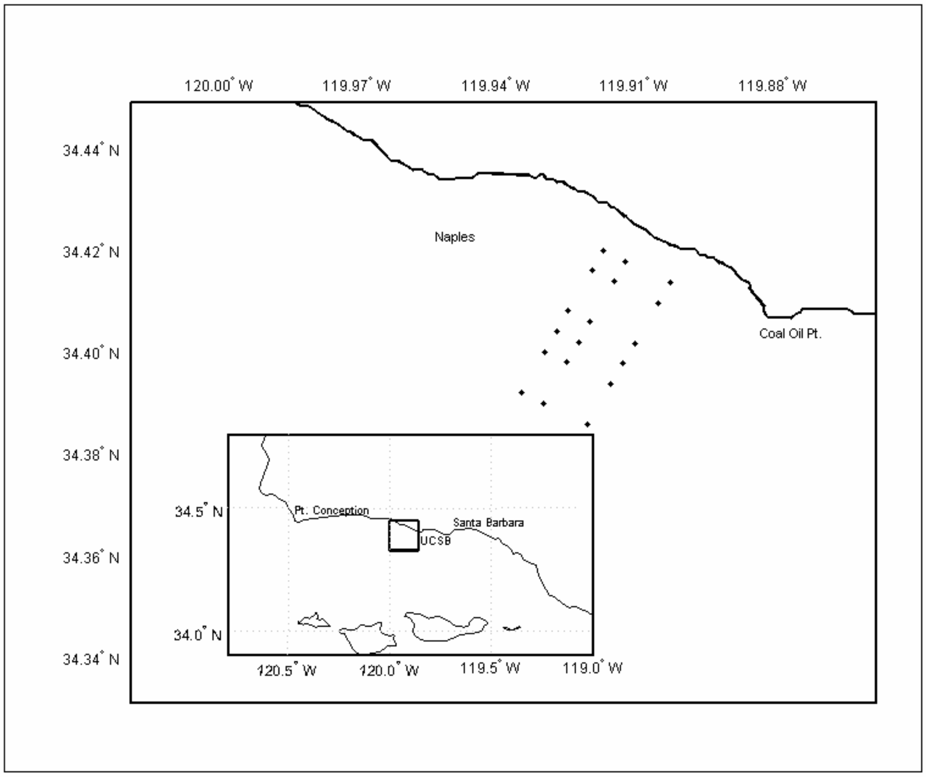

Figure 3. Map showing the location of the study area along with the deployment grids.

Two deployment grids are defined. The first (hereafter inner-shelf grid) is comprised of two irregularly spaced (1.5 by 1.5 km) 3 by 3 grids with 0.5 and 1 km spacing between adjacent stations (Figure 3). The two grids are spaced 0.5 km apart in the offshore direction. The second (hereafter HF radar grid) is a regularly spaced 5 by 5 grid located further offshore within a 2 by 2 km HF radar bin (0.5 km spacing). This is the location where HF radar radials that are orthogonal, and HF radar performance is expected to be optimal. Spacing for the first grid allows examination of spatial coherence for a variety of along-shore and across-shore distances. Spacing for the second grid allows for the uniform distribution of drifters within the HF radar grid cell.

3.2 Sampling scheme

After a series of test deployments during the instrument development period, 17 inner-shelf deployments were performed between14 November, 2002 and 2 December, 2003 (Table 2). Releases were originally planned for every three weeks but turned out to be irregularly spaced in time. Boat scheduling proved more difficult than expected, releases were cancelled due to rough conditions and a nonfunctional boat hoist, and the drifters were temporarily removed from service for a firmware upgrade and a subsequent rebuilding (17 July to 23 September). A total of 4 HF radar grid deployments occurred between 10 July 2003 and 24 August 2004. These deployments occurred during the summer months when conditions in the SBC were relatively calm.

Table 2. Data summary for each of the 17 inner-shelf and 4 HF radar grid drifter deployments.

deployment date	# drifters deployed	avg start time (UTC)	avg stop time (UTC)	avg u velocity (cm/s)	avg v velocity (cm/s)	avg along shore velocity (cm/s)	avg across shore velocity (cm/s)
11/14/2002	5	18:10	20:00	-4.47	12.25	-8.28	10.09
3/3/2003	13	18:00	23:34	-11.37	5.01	-12.17	1.03
4/11/2003	10	16:00	21:20	-18.33	16.70	-20.98	8.19
4/17/2003	12	17:00	21:10	-10.81	15.09	-13.42	11.68
4/24/2003	8	16:40	20:50	3.62	12.48	-1.48	12.75
5/22/2003	15	16:40	22:50	-9.48	12.77	-10.94	8.72
6/4/2003	1	18:20	20:50	-30.71	11.99	-32.59	-3.34
6/9/2003	16	16:10	19:50	4.34	4.35	2.25	5.71
6/19/2003	13	16:00	21:30	-3.88	5.51	-5.60	3.84
6/26/2003	9	15:40	21:00	1.36	4.77	-0.47	4.96
7/17/2003	7	15:43	20:30	-6.45	5.21	-7.26	3.01
9/23/2003	8	16:50	21:50	0.72	5.77	-1.62	5.48
9/30/2003	9	16:10	21:30	-30.36	10.36	-30.33	-0.54
10/14/2003	9	16:20	21:30	-19.47	15.71	-21.86	8.48
10/28/2003	10	17:40	23:40	-20.60	7.162	-20.74	1.06
11/25/2003	14	17:30	23:20	-11.69	10.15	-13.87	5.50
12/2/2003	12	17:10	21:40	-3.41	5.34	-5.05	3.66

7/10/2003	18	16:20	21:49	-25.61	29.61	-30.13	24.00
7/19/2004	31	15:20	22:50	-11.07	19.88	-13.63	17.95
8/12/2004	30	16:20	22:20	-19.09	14.76	-20.46	11.86
8/24/2004	23	15:50	21:32	-2.81	16.79	-5.75	16.11

For the inner-shelf grid deployments, drifters were generally released between 0800 and 0930 local time and recovered between 1200 and 1500 local time. The short sampling durations were required to recover drifters before they entered the surf zone and washed ashore. For the HF radar grid deployments, drifters were also deployed in the morning. As they exited the 2 by 2 km HF radar grid, they were picked up and redeployed at the stations furthest from the other drifters, so as to keep a mostly uniform spatial distribution in the box. Typically 2 or 3 drifters were picked up at a time and redeployed at the upstream edge of the box. Each drifter was redeployed roughly twice during each 5 to 7 hour experiment. The inner-shelf and HF radar grid experiments resulted in a total of 171 and 128 drifter tracks, respectively.

4. Results

4.1 Drifter tracks

The purely descriptive view of the local circulation as inferred from the complete set of inner-shelf drifter trajectories shows that currents are almost always moving in the up-coast direction, and mostly in the on-shore direction (Figure 4). Interestingly, this occurs despite the prevailing winds being from the northwest, opposite the general direction of drifter movement. 149 of the 171 inner-shelf drifter tracks moved into shallower water during their deployment periods. The propensity for cross-shore movement, relative to along-shore motion, is greatest in the HF radar deployment grid and then again very near the shore. The former is consistent with the presence of a mid-basin cyclonic gyre, or the “cyclonic” regime reported by Oey et al (2001). The latter is likely due to wave-stress forcing which becomes more pronounced with decreased depth. For the inner-shelf deployments, track lengths tend to increase with distance from the shore indicating the weakest velocities nearest the coast. The overall picture suggests that the local circulation is not a simple balance between surface and bottom stress, but that pressure and/or Coriolis forces may play a significant role.

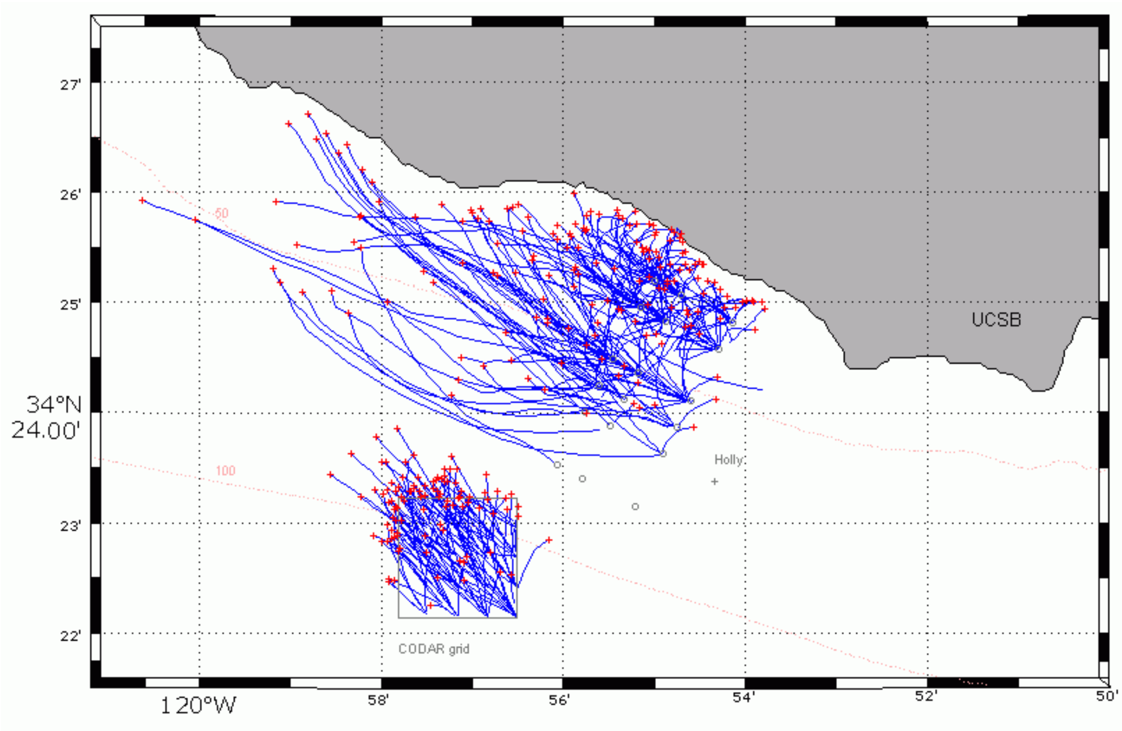

Figure 4. The complete set of drifter tracks collected.

Sets of tracks collected contemporaneously indicate the sorts of high frequency variations in currents that exist in the region. On 2 December, 2003, drifters move somewhat coherently, but the closer to shore a drifter, the more its track is oriented in the cross-shore direction (Figure 5a). Tracks collected on 11 April, 2003, show significantly greater velocities away from the coast (Figure 5b). Pronounced differences in the circulation can exist across distances of a km or less (Figure 5c; 17 July 2003), and velocities can change abruptly in time (Figure 5d; 26 June 2003). Maps showing trajectories for each of the individual deployment days are on the web at http://www.icess.ucsb.edu/~kirk/drifter/SBCIS/index_deployments.htm. In general, daily tracks demonstrate a variety of high-frequency small-scale motions that exist in the region.

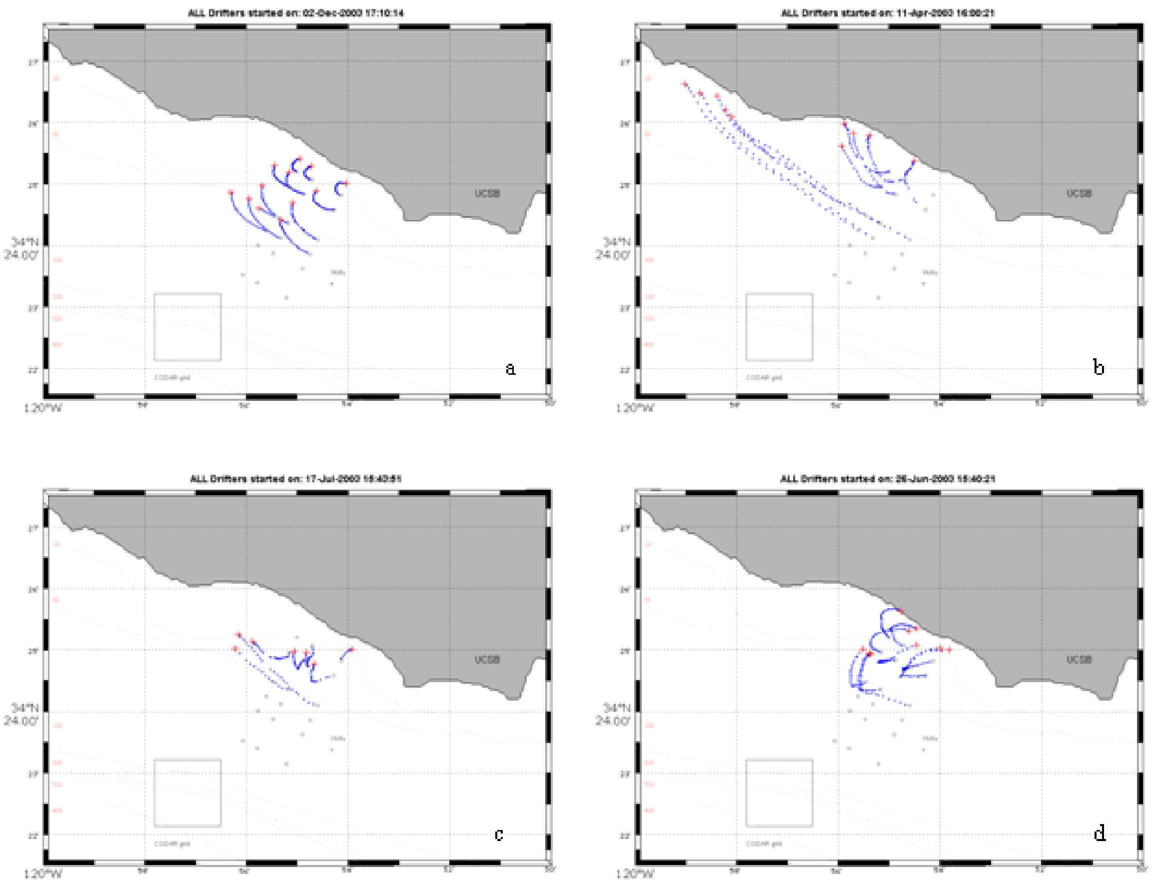

Figure 5. Drifter tracks collected on a) 2 December, 2003, b) 11 April, 2003, c) 17 July, 2003, and d) 26 June, 2003.

4.2 Velocity Statistics

Mean velocities and their corresponding deviations have been computed on a 0.75 km grid as follows. Velocities were determined from a first difference in drifter positions at the midpoint between successive position records. Velocity values were then grouped in square bins and statistics computed for bins with observations on at least 5 sampling days. This arbitrary threshold was selected to eliminate statistics computed from observations collected during a limited time, and to give results over the course of several synoptic events. Mean vectors are included with variance ellipses to identify variations with distance from shore and quantify the high frequency variations indicated above. They do not depict accurate annual averages.

Mean velocity vectors range from 3.5 to 34.5 cm s^{-1} and are mostly oriented parallel to the straight section of coast between the Coal Oil and Naples headlands (Figure 6a). There are two notable exceptions. Within 1 km of the coastline, mean velocities are mostly directed onshore, presumably following wave stress forcing. Between roughly 1.5 and 2.5 km offshore, velocities are also directed in the onshore direction. This is a function of the deployment scheme. No drifters are deployed in this region. Drifters enter from either offshore or onshore only during times of cross-shore flow, and therefore possess a sampling bias. The mean field also shows a general increase in velocity with distance offshore. In general, mean velocities are in direct opposition to the local wind stress suggesting the importance of pressure forces in driving the local circulation.

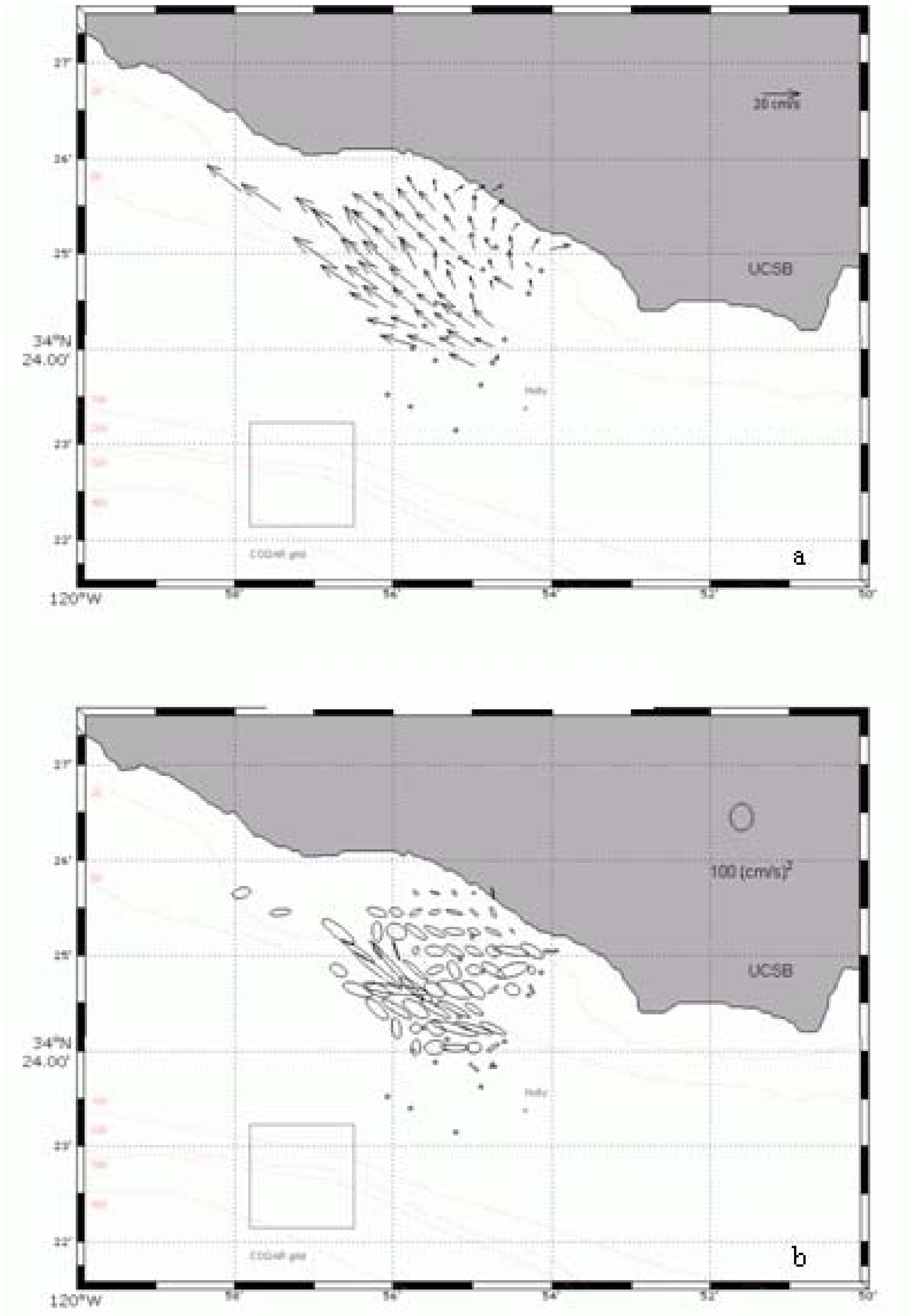

Figure 6. Velocity statistics computed for 0.75 km x 0.75 km bins in which data was collected during at least 5 different days. a) Mean velocity vectors, and b) associated variance ellipses.

Variance ellipses associated with the mean values are illustrated in Figure 6b. The ellipses vary in size, eccentricity, and orientation indicating the inhomogeneous nature of the flow field in the study region. Major axis length ranges from 18 to 323 $cm^2 s^{-2}$ with the largest values generally existing in the offshore region. Ellipses near the coast are smaller, but with similar eccentricity and along bathymetry orientation. The large eccentricity ellipses near the 50 m isobath arise from flow associated with a strong localized along-shore jet that occasionally occurs. In general, the ellipses indicate the magnitude of the along-shore velocity component to be the largest source of temporal variability. Pronounced spatial variations in the time-varying flow also exist.

4.3 Lagrangian Statistics

Lagrangain time and length scales quantify how drifter movement is correlated with previous samples. Such information is useful for defining appropriate decorrelation scales for coastal ocean models, and for validating modeled trajectory statistics. The Lagrangian scales are based on the velocity covariance defined as

$$R_{ij}(\tau, T, t_0, x_0) = \frac{1}{T} \int_{t_0}^{t_0+T} u_i'(x_0, t)\, u_j'(x_0, t+\tau)\, dt \qquad (1)$$

where $u_i'(x_0, t)$ is the velocity residual, at time t, for the i^{th} drifter track that passes through the point x_0 at time t_0, $u_j'(x_0, t+\tau)$ is the velocity residual at time $t+\tau$ for the j^{th} track that passes through x_0 at time t_0, and T is the total integration time. Lagrangian integral time (T_i^L) and length (L_i^L) scales for a single track i are then

$$T_i^{\,L} = \int_0^{t} R_{ii}(\tau)\, dt \qquad (2)$$

$$L_i^{\,L} = \, < u_i'^2 >^{1/2} \int_0^{t} R_{ii}(\tau)\, dt \qquad (3)$$

where $< u_i'^2 >$ is the velocity variance for track i, and integration is to the first zero crossing following Poulain and Niiler (1989).

Mean Lagrangian autocovariance curves computed from all tracks with lengths greater than 180 minutes show along-shore velocity observations decorrelate smoothly reaching zero between 90 and 100 minutes (Figure 7a). The along-shore curve continues to decrease until it reaches a value of -0.19 at 160 minutes, and then increases back toward zero. The region of negative correlation may be suggestive of eddy motions where along-shore flow in one direction occurs for roughly two hours followed by return flow in the opposite direction during the next (roughly) two hours (~120 to 250 minutes). After a period of near 4 hours the drifter has moved out of the eddy into a different (and uncorrelated) transient feature. Across-shore velocity observations decorrelate smoothly over a slightly longer time, reaching zero at a lag between 130 and 140 minutes (Figure 7b). Across-shore autocovariance values do not display negative values beyond -0.03. If the along-shore autocovariance curves indeed point to return flows associated with eddies, then the across-shore curves indicate the eddies are oriented mainly in the along-shore direction.

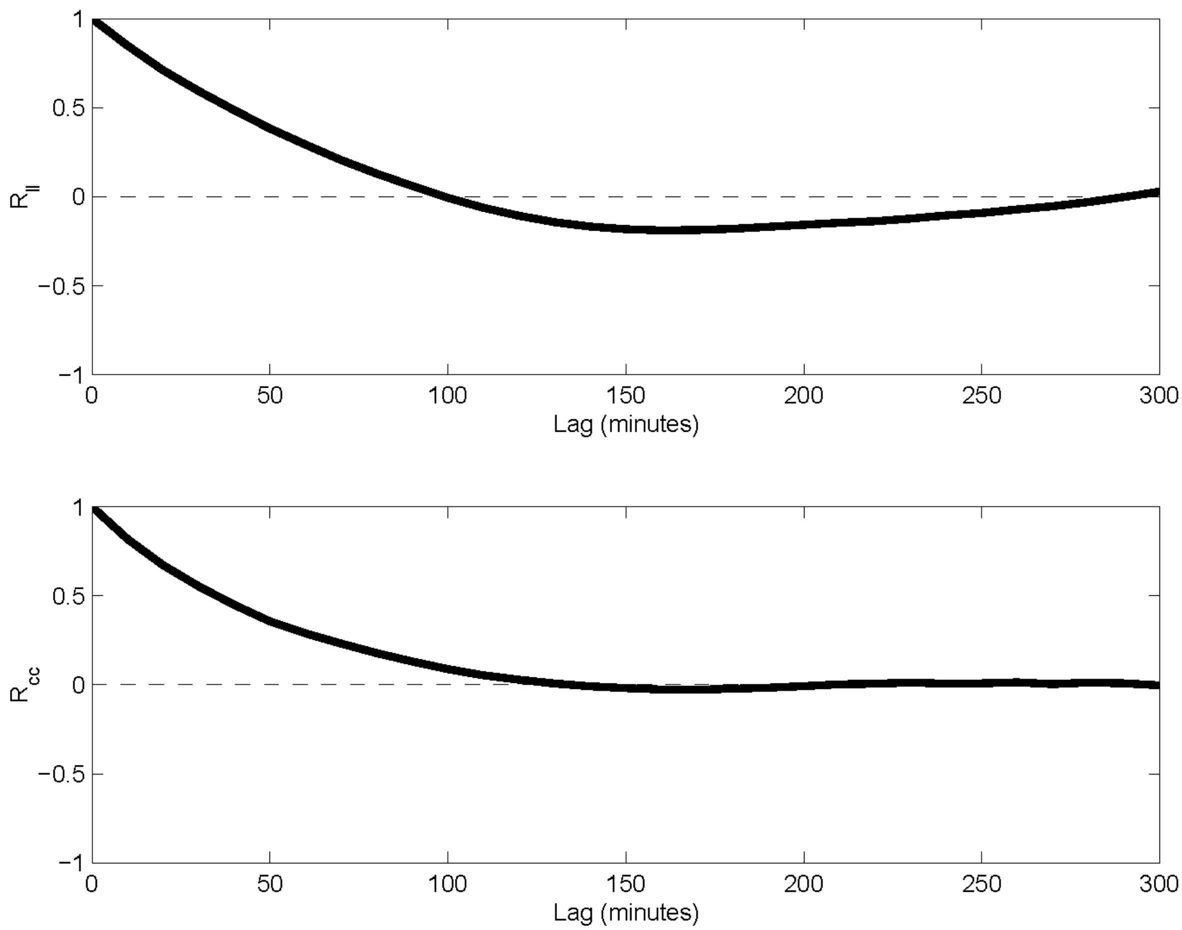

Figure 7. Mean autocovariance carves for the a) along-shore, and b) across-shore velocity components.

Decorrelation time scales for the along- and across-shore components are 42 and 43 minutes, respectively. Corresponding decorrelation length scales are 0.10 and 0.08 km, respectively. These scales are significantly shorter than those reported by Dever et al. (1998) for the basin scale circulation (1 day and 10 km). This is partly attributable to the enhanced velocity fluctuations that occur nearer the shore, but also to the higher frequency sampling rates and much shorter overall track lengths in the present study. It is possible that significant correlations exist on scales beyond the reported range, but they are not discernable with the existing data.

4.4 Dispersion Statistics

Mean squared dispersion has been computed by selecting all inner-shelf drifter pairs that come within 250 m and computing their subsequent separation (squared) in both the along- and across-shore directions (Figure 8). The 250 m threshold was arbitrarily selected to give close proximity while also allowing sufficient leeway so that at least 25 drifter pairs are used in the computation. Since initial spacing is greater than 250 m, pairs included in the analysis originally converged. Mean squared dispersion in both the along- and across-shore directions is surprisingly similar. Separation grows to ~0.02 km^2 after 40 minutes, and to 0.20 km^2 after 240 minutes. Dispersion follows a power law during the first 40 minutes and then grows as a linear function of time between 40 and 240 minutes. The sharp increase after 240 minutes is an artifact of a limited number of pairs extending that far in time, and the fact that once drifters are sufficiently separated they can be in extremely different flow regimes. After 240 minutes, one drifter has typically moved near the shore and is moving at a few cm s^{-1}, and the other (in the pair) is still offshore moving at > 10 cm s^{-1}. At first glance, the inner-shelf dispersion on such small scales does not closely follow Taylor (1921). This will be investigated in a more complete analysis of dispersion which is forthcoming.

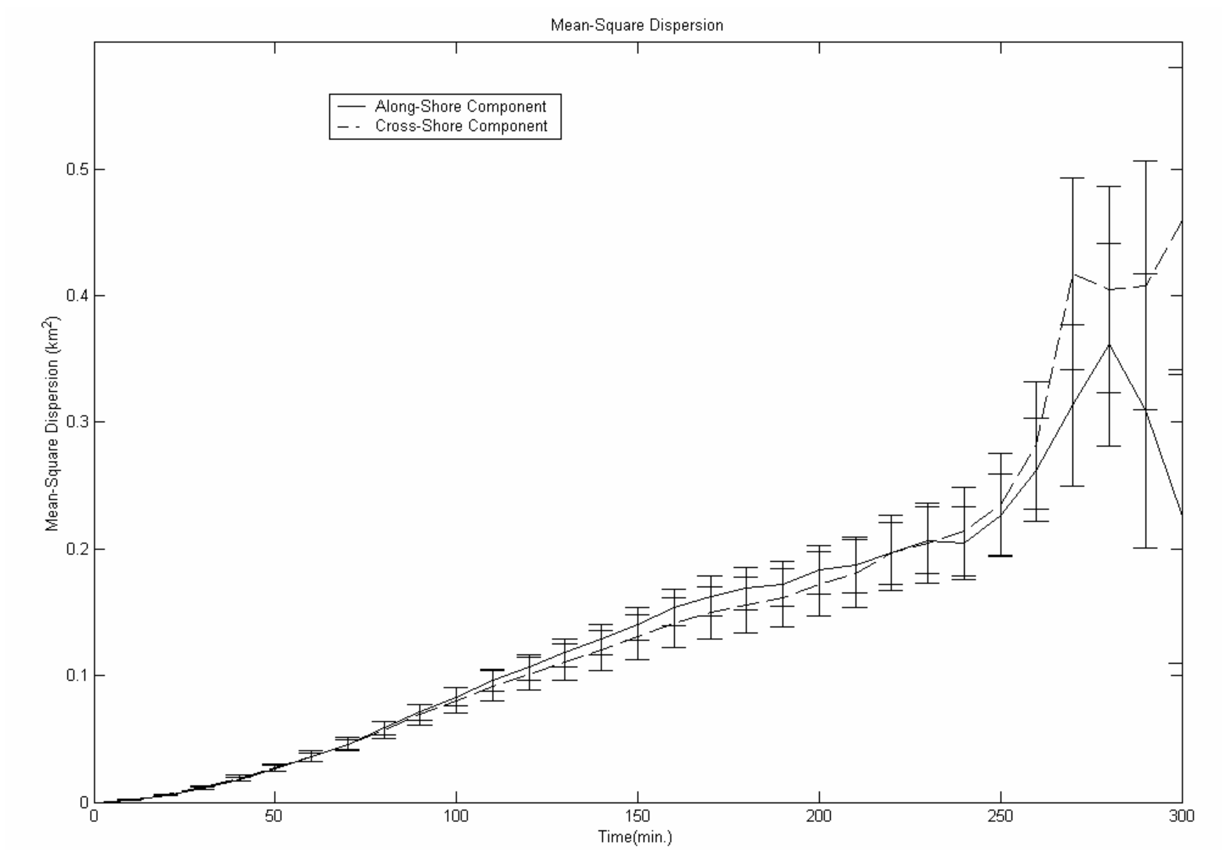

Figure 8. Mean squared dispersion in both the along-shore and across-shore directions. Error bars show standard deviations.

4.5 Comparison with HF radar derived velocities

High frequency radar systems have become a popular means of obtaining surface current data near the coast. HF radars use a Doppler technique to measure currents in the radial direction from each instrument. Radials must then be smoothed by averaging. Typical HF radar data are presented as hourly average velocities on a spatial grid near 1 to 2 km square, depending on radar frequency and radial averaging radii. HF radar coverage typically begins somewhere on the shelf and reaches the horizon.

HF radar results have a demonstrated accuracy of near 10 cm/s (Paduan and Rosenfeld 1996, Chapman and Graber 1997, Emery et al. 2004). Validation has occurred through comparison of HF radar data that are space and time averages against data from a single current meter that is only a time average. Existing comparisons with drifter derived velocities use few tracks so averaging is over the limited locations and times of drifter sampling, and not the same space and time domains used to compute average HF radar values. Meaningful validation of HF radar velocities requires comparison with measurements made on commensurate time and space scales.

The HF radar grid sampling gives up to 41 velocity observations distributed throughout a 2 km square HF radar grid cell in an hour. This space-time resolution can offer a much improved validation of 2 km, hourly average, HF radar velocities. Comparison of drifter and HF radar derived velocities when there is at least 1 drifter velocity observation in the HF radar (time/space) bin gives root mean square (rms) errors of 9.8 and 9.9 cm s^{-1} for the east-west (u; mainly alongshore) and north-south (v; mainly across-shore) velocity components, respectively (Figure 9a). As the number of drifter velocity observations within each 2 km bin for a given hour increases, the rms velocity error decreases. For time and space bins when there are at least 34 drifter derived velocity observations, the rms velocity error decreases to 6.7 and 6.1 cm s^{-1} for the u and v velocity components, respectively.

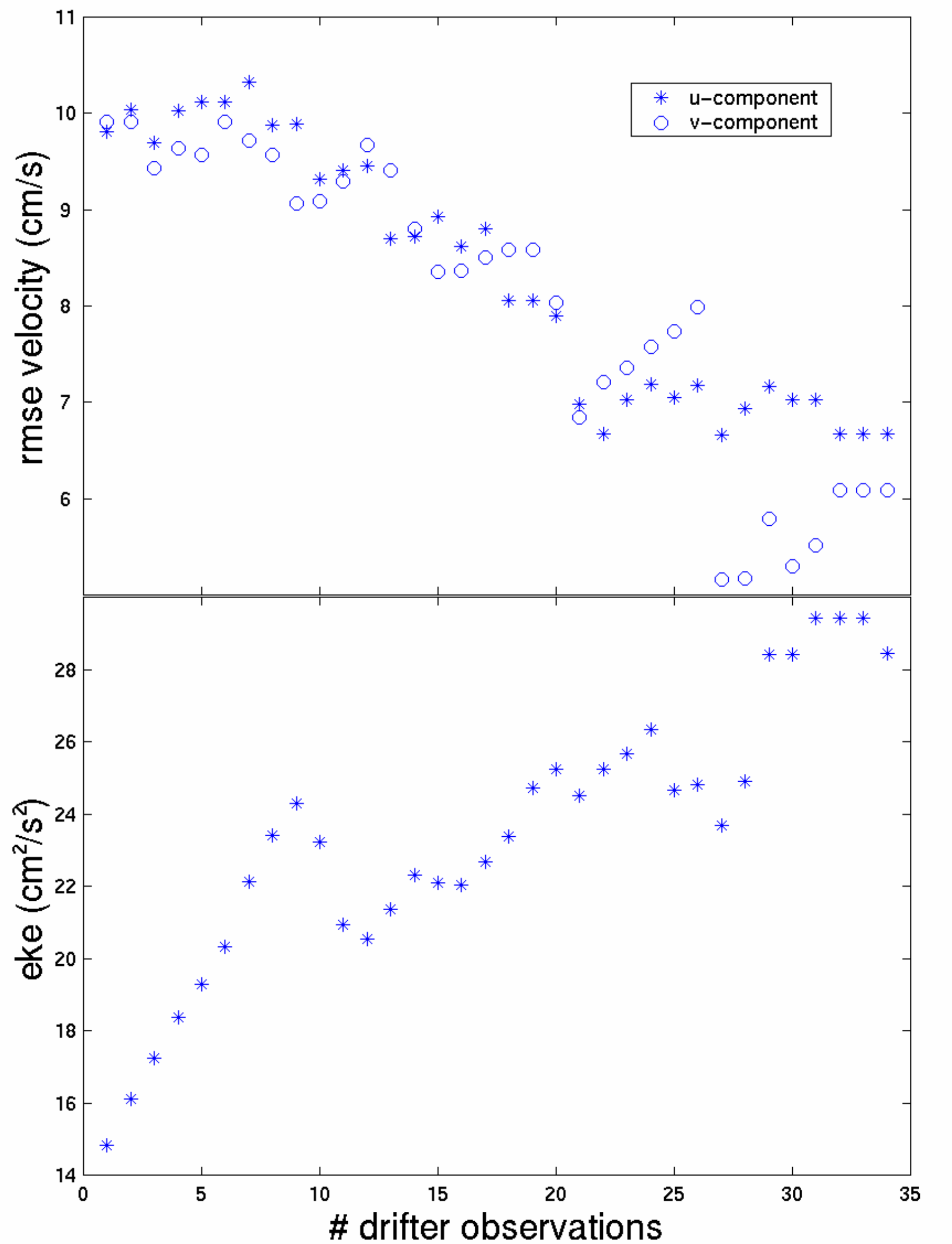

Figure 9. Root mean squared error (RMSE) between HF radar and drifter derived average velocity components (top). Average velocities are over 2 km square bins and 1 hour. RMSE is computed using average velocities where at least *x* drifter observations are used to calculate the average. The u velocity component is east-west and mostly along-shore in the study region. The v component is north-south and mostly across-shore. Associated eddy kinetic energy (EKE) on from drifter data (bottom). EKE is computed as $0.5*(\langle u'u'\rangle + \langle v'v'\rangle)$ where u' and v' give deviations from the average u and v velocities, respectively, and the angle brackets denote mean quantities. EKE is computed separately for each time (1 hour) and space (2 km grid) bin. Data for two days that give a relatively large contribution to a single space bin were removed to avoid spatial biasing.

This simple performance analysis suggests that previous validations may have overstated HF radar error near 50%, or ~3 to 4 cm s^{-1}, by failing to resolve the same time-space motions which are included in typical 2 km square and 1 hour HF radar averages. More importantly, the analysis indicates that coastal flows are highly variable on (time and space) scales shorter than typically resolved with HF radar data. Eddy kinetic energy (EKE), computed as $0.5 * \left\langle u'^2 + v'^2 \right\rangle$, where u' and v' are the fluctuating components of the east-west and north-south velocity components, respectively, and the brackets denote a mean, is 15.1 cm^{-2} s^{-2} when computed on spatial scales less than 2 km, and hour time scales, with all the HF radar grid data (Figure 9b). EKE increases 67%, to 25 cm^{-2} s^{-2} when computed for times when there are at least 25 drifter observations within the grid. The number of observations within a grid cell needs to be increased in future experiments to determine the asymptotic value of EKE. Such a value is of interest for tuning models to produce realistic values of eddy energy.

4.6 Comparison with HF radar derived trajectories

Tracks computed from 2 km hourly average Eulerian HF radar fields, using a fourth order Runge-Kutta integration scheme, are compared with observed drifter tracks. Mean separation distances for the east-west (mainly alongshore) and north-south (mainly across-shore) directions, are computed every 10 minutes (Figure 10). Mean east-west separation grows to -65 m after 60 minutes, to -273 m after 120 minutes and to -673 m after 240 minutes. The negative values indicate that trajectories computed from HF radar derived trajectories are moving faster in the westward direction than the drifters. Mean north-south separation grows at almost the same rate out to 90 minutes and then begins to grow faster. The mean north-south separations at 120 and 240 minutes are -358 m and -1260 m, respectively, indicating the HF radar derived trajectories move slower in the onshore direction.

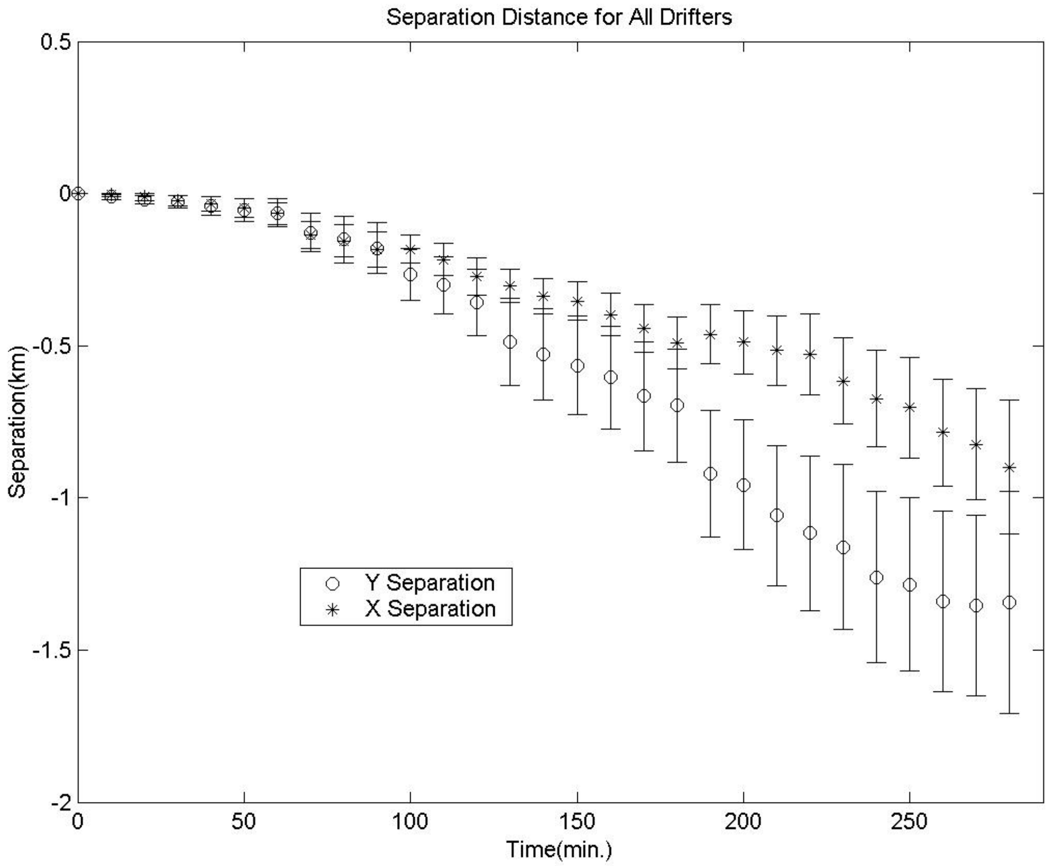

Figure 10. Average separation distance (with standard error) between observed drifter tracks and tracks computed with HF radar derived velocities as a function of time. The HF radar tracks are computed from hourly average velocities on a 2 km grid using fourth order Runge-Kutta integration. The number of track pairs used to compute a mean varies from 88 (at 10 minutes) to 9 (at 280 minutes), and decreases fairly linearly.

Although comparisons between HF radar and drifter derived velocities show improved agreement, there are still significant discrepancies in trajectories. Significant directional biases and a larger difference in the across-shore component exist. Such results indicate that an optimum sub-grid-scale-model for rectifying trajectory discrepancies should not simply be isotropic. If an HF radar derived trajectory were to be used to assist an at-sea search, results suggest that the lost object would most likely be located to the east, and onshore of the position given by the computed trajectory. Additional comparisons, and more thorough quantitative analyses, are necessary to develop sub-grid-scale parameterizations in terms of location, flow properties, and HF radar sampling characteristics. This will ultimately increase the accuracy of trajectories computed with HF radar data.

References

Beckenbach E., and L. Washburn. 2004. Low-frequency waves in the Santa Barbara Channel observed by high-frequency radar. *Journal of Geophysical Research,* **109**:2010-2038

Brink, K.H. and R.D. Muench. 1986. Circulation in the Point Conception – Santa Barbara Channel region. *Journal of Geophysical Research*, **91**:877-895

Chapman R.D. and H.C. Graber. 1997. Validation of HF radar measurements. *Oceanography*, **10(2)**:76-79

Davis, R.E. 1985. Drifter observations of coastal surface currents during CODE: The method and descriptive view. *Journal of Geophysical Research*, **90**:4741-4755

Dever, E.P., M.C. Hendershott, and C.D. Winant. 1998. Statistical aspects of surface drifter observations of circulation in the Santa Barbara Channel. *Journal of Geophysical Research*, **103**:24,781-24,797

Dorman, C.E. and C.D. Winant. 2000. The structure and variability of the marine atmosphere around the Santa Barbara Channel. *Journal of Geophysical Research*, **128**:261-282

Emery, B.M., L. Washburn, M. Love, M.M. Nishimoto, and J.C. Ohlmann. Do oil and gas platforms off California reduce recruitment of bocaccio (*Sebastes paucispinis*) to natural habitat? An analysis based on trajectories derived from high frequency radar, *Fisheries Bulletin*, (In review) 2004.

Graber, H.C., B.K. Haus, R.D. Chapman, and L.K. Shay. 1997. HF radar comparison with moored estimates of current speed and direction: Expected differences and implications, *Journal of Geophysical Research*, **102(C8)**:18,749-18,766

Harms, S. and C.D. Winant. 1998. Characteristic patterns of circulation in the Santa Barbara Channel. *Journal of Geophysical Research,* **103**:3041-3065

Kolpack, R.J. 1971. Biological and Oceanographical Survey of the Santa Barbara Channel Oil Spill 1969-1970, **2**, 477pp., Allen Hancock Foundation, University of Southern California, Los Angeles

Lenz, S.J. 1994. Current dynamics over the northern California inner shelf. *Journal of Physical Oceanography*, **24**:2461-2478

Lenz, S.J. and C.D. Winant. 1986. Subinertial currents on the southern California shelf. *Journal of Physical Oceanography*, **16**:1737-1750

Niiler, P.P, A.L. Sybrandy, K.Bi, P.M. Poulain, and D. Bitterman. 1995. Measurements of the water following capability of holey-sock and TRISTAR drifters, *Deep Sea Research*, **42**:1951-1964

Oey, L.Y., D.P. Wang, T. Hayward, C. Winant, and M. Hendershott. 2001. “Upwelling” and “cyclonic” regimes of the near-surface circulation in the Santa Barbara Channel. *Journal of Geophysical Research*, **106**:9213 – 9222

Ohlmann, J.C., P.F. White, A.L. Sybrandy, and P.P. Niiler. GPS-Cellular drifter technology for coastal ocean observing systems. *Journal of Atmospheric Oceanic Technology*, in press.

Poulain, P.M. and P.P. Niiler. 1989. Statistical analysis of the surface circulation in the California Current system using satellite-tracked drifters. *Journal of Physical Oceanography*, **19**:1588-1603

Paduan, J.D. and L.K. Rosenfeld. 1996. Remotely sensed surface currents in Monterey Bay from shore-based HF radar (CODAR). *Journal of Geophysical Research*, **101**:20,669-20,686

Taylor, G.I. 1921. Diffusion by continuous movements. *Proceedings of the London Mathematical Society.* **A20**:196-211

Winant, C.D., D.J. Alden, E.P. Dever, K.A. Edwards, and M.C. Hendershott. 1999. Near-surface trajectories off central and southern California. *Journal of Geophysical Research,* **104**:15,713 – 15,726

Winant, C.D., E.P. Dever, and M.C. Hendershott. 2003. Characteristic patterns of shelf circulation at the boundary between central and southern California. *Journal of Geophysical Research*, **108**:3021 – 3034

The Department of the Interior Mission

As the Nation's principal conservation agency, the Department of the Interior has responsibility for most of our nationally owned public lands and natural resources. This includes fostering sound use of our land and water resources; protecting our fish, wildlife, and biological diversity; preserving the environmental and cultural values of our national parks and historical places; and providing for the enjoyment of life through outdoor recreation. The Department assesses our energy and mineral resources and works to ensure that their development is in the best interests of all our people by encouraging stewardship and citizen participation in their care. The Department also has a major responsibility for American Indian reservation communities and for people who live in island territories under U.S. administration.

The Minerals Management Service Mission

As a bureau of the Department of the Interior, the Minerals Management Service's (MMS) primary responsibilities are to manage the mineral resources located on the Nation's Outer Continental Shelf (OCS), collect revenue from the Federal OCS and onshore Federal and Indian lands, and distribute those revenues.

Moreover, in working to meet its responsibilities, the **Offshore Minerals Management Program** administers the OCS competitive leasing program and oversees the safe and environmentally sound exploration and production of our Nation's offshore natural gas, oil and other mineral resources. The MMS **Royalty Management Program** meets its responsibilities by ensuring the efficient, timely and accurate collection and disbursement of revenue from mineral leasing and production due to Indian tribes and allottees, States and the U.S. Treasury.

The MMS strives to fulfill its responsibilities through the general guiding principles of: (1) being responsive to the public's concerns and interests by maintaining a dialogue with all potentially affected parties and (2) carrying out its programs with an emphasis on working to enhance the quality of life for all Americans by lending MMS assistance and expertise to economic development and environmental protection.